Effects of Extension or Prevention of π-Conjugation on Photoinduced Electron Transfer Processes of Ferrocene−Oligothiophene−Fullerene Triads

Takumi Nakamura,[†] Hiroki Kanato,[‡] Yasuyuki Araki,[†] Osamu Ito,*[,†] Kazuo Takimiya,[‡] Tetsuo Otsubo,*[,‡] and Yoshio Aso[§]

Institute of Multidisciplinary Research for Advanced Materials, Tohoku University, Katahira, Aoba-ku, Sendai, 980-8577, Japan, Department of Applied Chemistry, Graduate School of Engineering, Hiroshima University, Higashi-Hiroshima 739-8527, Japan, and The Institute of Scientific and Industrial Research, Osaka University, Ibaraki, Osaka 567-0047, Japan

Received: November 8, 2005; In Final Form: January 17, 2006

Photoinduced electron-transfer processes of alkyl-inserted ferrocene−trimethylene−oligothiophene−fullerene (Fc-tm-*n*T-C_{60}) linked triads and directly linked ferrocene−oligothiophene−fullerene(Fc-*n*T-C_{60}) triads were investigated using time-resolved fluorescence and transient absorption spectroscopic methods. In nonpolar solvent, the energy-transfer (EN) process occurred from ^1nT* to C_{60} for both triads, without forming the charge-separated (CS) state. In polar solvent, the initial CS state, Fc-tm-nT$^{\bullet+}$-$C_{60}^{\bullet-}$, was formed via Fc-tm-*n*T-$^1C_{60}$* after the EN process from ^1nT* by photoexcitation of the *n*T moiety and after direct photoexcitation of the C_{60} moiety. For Fc-tm-nT$^{\bullet+}$-$C_{60}^{\bullet-}$, the positive charge shifted from the nT$^{\bullet+}$ moiety to the Fc moiety, producing the final CS state, Fc$^{\bullet+}$-tm-*n*T−$C_{60}^{\bullet-}$, which lasted for 22−330 ns by changing *n*T from 4T to 12T. For Fc-*n*T-C_{60} in polar solvent, the CS state, in which the radical cation is delocalized on both Fc and *n*T moieties ((Fc-*n*T)$^{\bullet+}$-$C_{60}^{\bullet-}$), was formed immediately after direct photoexcitation of the *n*T and C_{60} moieties. The lifetimes of (Fc-*n*T)$^{\bullet+}$-$C_{60}^{\bullet-}$ were estimated to be 0.1−50 ns by changing *n*T from 4T to 12T. The longer lifetimes of Fc$^{\bullet+}$-tm-*n*T-$C_{60}^{\bullet-}$ than those of (Fc-*n*T)$^{\bullet+}$-$C_{60}^{\bullet-}$ are caused by the insertion of the trimethylene chain to prevent the π-conjugation between the Fc and *n*T moieties. The lifetimes for Fc$^{\bullet+}$-tm-*n*T-$C_{60}^{\bullet-}$ and (Fc-*n*T)$^{\bullet+}$-$C_{60}^{\bullet-}$ are prolonged by changing *n*T from 4T to 12T. For the charge-recombination process of Fc$^{\bullet+}$-tm-*n*T-$C_{60}^{\bullet-}$, the damping factor was evaluated to be 0.10 Å^{-1}. For (Fc-*n*T)$^{\bullet+}$-$C_{60}^{\bullet-}$, the oxidation potentials of the *n*T moieties control the electron-transfer process with reflecting stabilization of the radical cations of the *n*T moieties.

Introduction

The conjugated nanoscale molecules are useful to design the molecular electronic devices (i.e., electric luminescent devices,[1] photovoltaic cells,[2] field-effect transistors,[3] nonlinear optics,[4] and electrical conductors[5]). Recently, the photoinduced electron transfer (ET) systems with highly efficient charge-separation (CS) and slow charge-recombination (CR) processes have been applied to the photovoltaic cells.[2] Highly conjugated molecular wires are indispensable for molecular electron devices.[5] Oligothiophenes (*n*Ts) seem to be one of the most well-investigated π-conjugated oligomers,[6−8] because of their remarkable characteristics such as a rigid rodlike structure.

On the other hand, fullerenes are one of the well-investigated molecules;[9] in particular, C_{60} was widely used for electron-transfer systems as an electron acceptor.[10] We previously reported that photoexcited fullerenes (C_{60} or C_{70}) accept electron from *n*Ts, when they are mixed in polar solvents;[11] it was revealed that the intermolecular ET process occurs via the triplet-excited states of fullerenes and *n*Ts, depending on the wavelength of the irradiated light. More recently, the efficient CS process was reported to occur in the covalently bonded oligothiophene−C_{60} dyads.[12] The CS process happens efficiently via the singlet excited states of the *n*Ts and C_{60}. The CR processes occur with fast and slow components; from the slow decay, lifetimes of the radical ion pair (τ_{RIP}) of *n*T−C_{60} dyads were evaluated to be longer than 10^{-6} s in polar solvents, because the slow CR process of these dyads falls in the Marcus "inverted region".[13] We extended these studies by adding porphyrins at the terminal of the *n*T side in the *n*T−C_{60} dyads by synthesizing porphyrin−*n*T−C_{60} triads.[14] The photoinduced processes after the photoexcitation of the porphyrins in the triads have been predominantly studied, because of huge absorption in the visible region and appropriate fluorescence lifetimes of these porphyrins. Although the *n*T moieties in porphyrin-*n*T−C_{60} act as efficient molecular spacers for the CS process, they also act as hole traps for the stepwise CR process.

Ferrocene (Fc) is one of the interesting molecules for designing the photoinduced ET systems, because its very low oxidation potential (E_{ox}) is expected to serve the superior function as a good cation trap. Indeed, the extremely long CS state was confirmed in Fc−porphyrine−C_{60} linked molecules.[15]

In our previous paper, two types of triads were prepared; one is a trimethylene (tm)-inserted type (Fc-tm-*n*T-C_{60}) and another is the directly connected Fc-*n*T-C_{60} triad, in which π-conjugation is possible between the Fc moiety and the *n*T moiety, as shown in Figure 1.[16] In the present study, we examined the CS and CR processes, as well as the energy-transfer (EN) process, in

* Authors to whom correspondence should be addressed. E-mail addresses: ito@tagen.tohoku.ac.jp (O.I.), otsubo@hiroshima-u.ac.jp (T.O.).
[†] Tohoku University.
[‡] Hiroshima University.
[§] Osaka University.

10.1021/jp056436o CCC: $33.50
Published on Web 02/11/2006

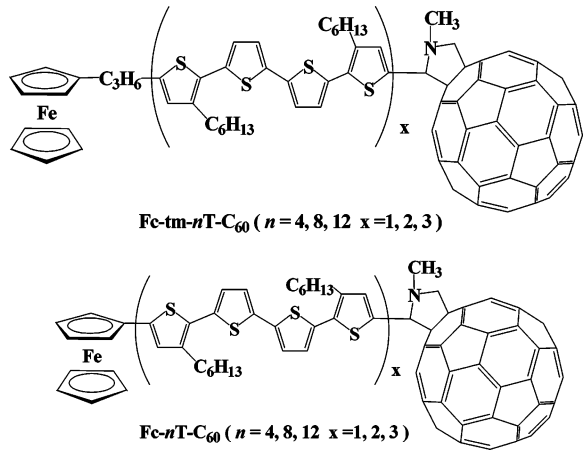

Figure 1. Molecular structures of Fc-tm-*n*T-C_{60} and Fc-*n*T-C_{60}.

Fc-tm-*n*T-C_{60} and Fc-*n*T-C_{60} by time-resolved absorption and fluorescence measurements after excitation of the *n*T and C_{60} moieties. To investigate the distance effect on the CS, CR, and EN processes, we compared three *n*Ts: 4T, 8T, and 12T. Moreover, the *n*T moieties are also expected to act as an electron donor. It is well understood that the E_{ox} values of the *n*T moieties decrease with their lengths, because the π-conjugation extended along the chain. For the rapid CS process via the excited states of the *n*T moieties, the sub-picosecond fluorescence and transient absorption measurements have been performed, whereas nanosecond transient absorption measurements in the visible and near-infrared regions were effectively used for the slow CR process.

Experimental Section

Materials. Fc-tm-*n*T-C_{60} and Fc-*n*T-C_{60} were synthesized by the methods described in the previous paper.[16] Components such as alkyl-substituted oligothiophenes (*n*T = 4T, 8T, and 12T) and *N*-methylpyrrolidino-C_{60} (NMPC_{60}) were prepared according to the methods described in the literature.[6,14a] Other chemicals such as Fc and solvents (benzonitrile (PhCN) and toluene) were of the best commercial grade available.

Methods. Steady-state absorption spectra were measured on a JASCO model V-530 UV/VIS spectrophotometer. Steady-state fluorescence spectra were measured on a Shimadzu model RF-5300 PC spectrofluorophotometer.

The fluorescence lifetimes of the C_{60} moieties in the triads were measured with a streak scope (Hamamatsu Photonics, model C4334-01) using a second-harmonic generation (SHG, 400 nm) of a Ti:sapphire laser (Spectra-Physics, model Tsunami 3950-L2S, with a full width at half maximum (fwhm) of 100 fs) as an excitation source.

Ultrafast fluorescence dynamics of the *n*T moieties in the triads were studied using a fluorescence upconversion method. The light source was a mode-locked Ti:sapphire laser (Spectra-Physics, model Tsunami 3950-L2S, fwhm = 100 fs) pumped with a diode-pumped solid-state laser (Spectra-Physics, model Millennia VIs J, operated at a power of 6.0 W). An 82-MHz pulse train with an average power of 1.0 W was produced by an oscillator in a fixed range at 800 nm. The fundamental pulse (λ = 800 nm) was used for a gate pulse in the upconversion process. The second-harmonic pulse (λ = 400 nm) was generated in a 0.4-mm-thick LiB_3O_5 (LBO) crystal, which was used for a pump beam for photoexcitation. To avoid polarization effect, the angle of the polarizations between the excitation and gate beams was set to the magic angle by a $\lambda/2$ plate. The fluorescence emitted from a sample was collected and focused into a 0.4-mm-thick β-BaB_2O_4 (BBO) crystal, which was mixed with the gate pulse with the crossing angle of ~9°. The fluorescence wavelength was selected by changing the phase-matching angle of the mixing crystal. The up-converted signals, which were spatially and spectrally separated from the other light, using a combination of an iris, an optical filter, and a monochromator, were detected using a photomultiplier tube (Hamamatsu, model R-4220P) with a photon counter (Stanford Research System, model SR400). The time resolution of measurements was estimated as 150 fs from the fwhm of the cross-correlation trace between the pump and gate pulses. A typical spectral window of fluorescence for our upconversion system was 420−640 nm.

Femtosecond transient absorption spectra were measured by the pump and probe method, using a Ti:sapphire regenerative amplifier seeded by the SHG of erbium-doped fiber laser (Clark-MXR CPA-2001 plus, 1 kHz, fwhm = 150 fs). A white continuum pulse that was used as a monitoring light was generated by focusing the fundamental of the amplifier on a rotating H_2O cell. The samples were excited by the pulsed laser light from a SHG (388 nm) of the fundamental laser pulse. The monitoring light transmitted through the sample in a rotating cell was detected with a dual MOS detector (Hamamatsu Photonics, model C6140) equipped with a polychromator and an InGaAs linear image sensor (Hamamatsu Photonics, model C5890-128) for detection of the near-IR region. A typical time resolution of the system was 200 fs.

Nanosecond transient absorption spectra were measured using the pulsed laser light from an optical parametric oscillation (Continuum Surelite OPO, fwhm = 4 ns) pumped by a Nd:YAG laser (Continuun, Surelite II-10). For the measurements of the transient absorption spectra in the near-IR region, a germanium avalanche photodiode (Hamamatsu Photonics, model B2834) was used as a detector for monitoring light from the pulsed xenon lamp.

Results and Discussion

Steady-State Absorption and Fluorescence Spectra. The absorption spectra of Fc-tm-*n*T-C_{60} and Fc-*n*T-C_{60} are shown in Figures 2a, 2b, and 2c for *n*T = 4T, 8T, and 12T, respectively, with those of the reference compounds in PhCN. The huge absorptions in the visible region were attributed to the *n*T moieties. In the case of Fc-tm-*n*T-C_{60}, the absorption spectrum was a simple superposition of the absorption bands of the constituents, revealing no interaction among the constituents in the ground state, because the π-conjugation between the *n*T moiety and the Fc moiety was prevented by the insertion of the tm spacer. On the other hand, the absorption band of the 4T moiety of Fc-4T-C_{60} has a tail extending to 600 nm and the peak position shifted to the red region, compared with the corresponding absorptions of 4T and Fc-tm-4T-C_{60}, indicating that the 4T moiety in Fc-4T-C_{60} is interacting with the Fc moiety. In the cases of the other Fc-*n*T-C_{60} (*n*T = 8T and 12T), the shift and broadening of the absorption bands of the *n*T moieties decrease with an increase in *n*T. These findings suggest that the *n*T moiety is strongly interacted with the Fc moiety in Fc-*n*T-C_{60}, although the extent of the interaction decreases as the *n*T moiety increases. In toluene, the absorption spectra were almost the same as those in PhCN.

Steady-state fluorescence spectra of Fc-tm-12T-C_{60} and Fc-12T-C_{60} observed with 420-nm light excitation in toluene are shown in Figure 3. The absorption intensities of the samples were matched at the excitation wavelength for the fluorescence measurements. The fluorescence peak at 560 nm is attributed

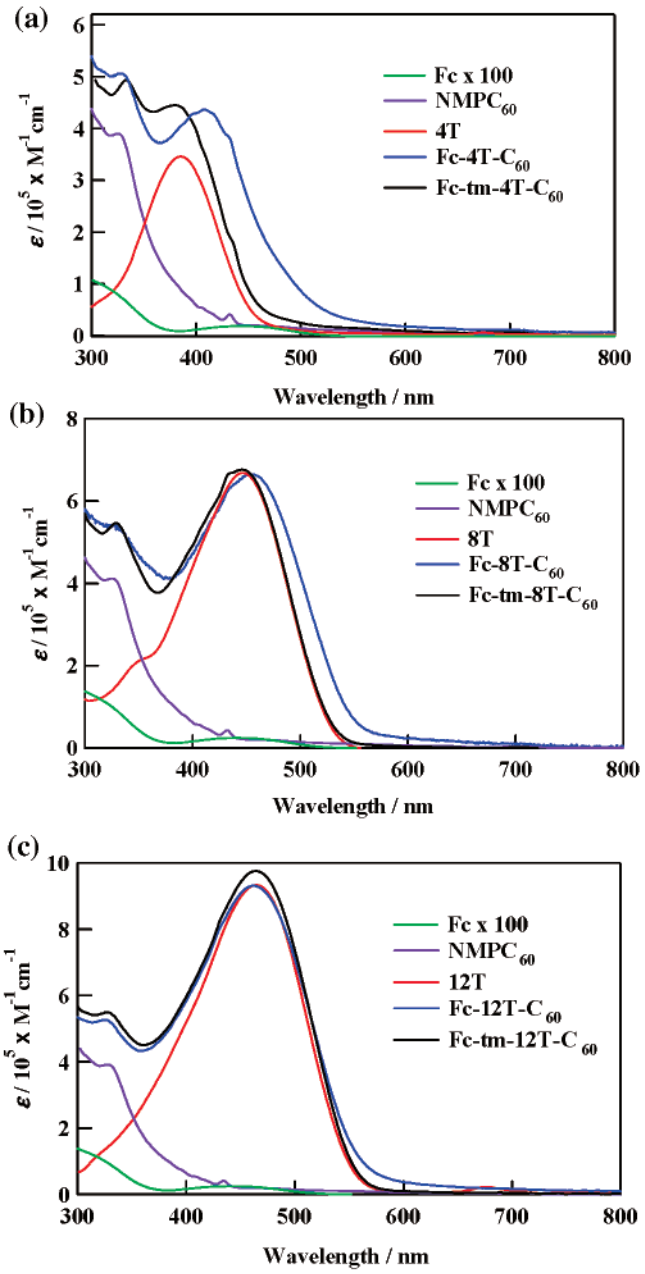

Figure 2. Absorption spectra of (a) Fc-tm-4T-C_{60} and Fc-4T-C_{60}, (b) Fc-tm-8T-C_{60} and Fc-8T-C_{60}, and (c) Fc-tm-12T-C_{60} and Fc-12T-C_{60} with reference compounds (Fc, $NMPC_{60}$, and *n*T) in PhCN.

to the 12T moiety, because the 420-nm light predominantly excited the 12T moiety. The fluorescence of the 12T moiety in Fc-tm-12T-C_{60} and Fc-12T-C_{60} was greatly quenched, compared with that of the reference (12T) with the fluorescence quantum yield of 0.4, as shown in Figure 3. For other Fc-tm-nT-C_{60} and Fc-*n*T-C_{60} materials, similar fluorescence quenching of the *n*T moiety was observed, compared with the corresponding *n*T with a fluorescence quantum yield (0.16 for 4T, 0.44 for 8T, and 0.52 for 12T).[11b] The bandwidth of the fluorescence in the 500−650 nm region of Fc-12T-C_{60} was broader than that of Fc-tm-12T-C_{60}, suggesting strong interaction between the 12T moiety and the Fc moiety, although the shift of the absorption bands was small. In the case of 4T, the fluorescence bandwidth in the 500−650 nm region of Fc-4T-C_{60} was almost the same as that of Fc-tm-12T-C_{60} (see the Supporting Information), although appreciable shift of the absorption band was observed. These observations suggest appreciable interaction between the *n*T moiety and the Fc moiety in the ground and excited states

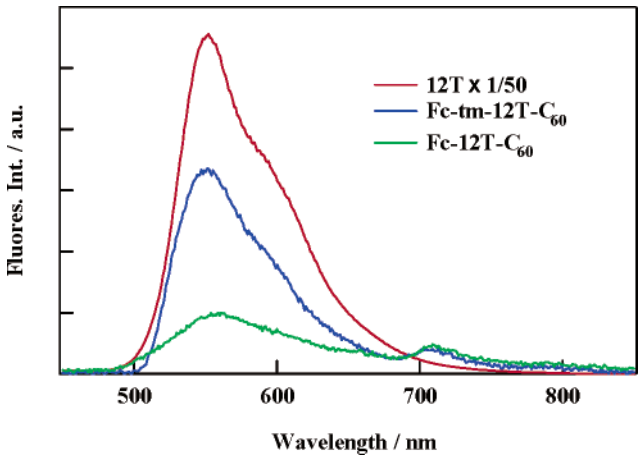

Figure 3. Steady-state fluorescence spectra of 12T, Fc-tm-12T-C_{60}, and Fc-12T-C_{60} in toluene with 420-nm light excitation. The absorption intensities of the samples were matched at the excitation wavelength for the fluorescence measurements.

of Fc-*n*T-C_{60}. Thus, the excited singlet state of Fc-*n*T-C_{60} should be described as ^{1}(Fc-*n*T)*-C_{60}.

The fluorescence due to the $^1C_{60}$* moiety appeared at 710 nm for Fc-tm-12T-C_{60}, indicating that the EN process occurred from the ^{1}12T* moiety to the C_{60} moiety. For other Fc-tm-*n*T-C_{60} materials, the appearance of fluorescence of the $^1C_{60}$* moiety due to the EN process was observed in toluene, because the excited singlet states of the *n*T moieties are all higher than that of the $^1C_{60}$* moiety. For Fc-*n*T-C_{60}, the fluorescence peak due to the $^1C_{60}$* moiety was similarly observed with appreciable fluorescence quenching of the *n*T moiety.

In PhCN, although fluorescence of the *n*T moiety was observed for Fc-tm-*n*T-C_{60} and Fc-*n*T-C_{60}, appreciable fluorescence intensity of the $^1C_{60}$* moiety was not observed. Absence of the fluorescence of the $^1C_{60}$* moiety suggests that the CS process occurs via the $^1C_{60}$* moiety, even though the $^1C_{60}$* moiety is produced via the ^{1}*n*T* moiety by the EN process.

Fluorescence Lifetime of *n*T in Triad. Figure 4a shows the time-dependent fluorescence intensities of the 12T moiety in Fc-tm-12T-C_{60} in toluene, which were measured by the upconversion method. The fluorescence time profile of Fc-tm-^{1}12T*-C_{60} was curve-fitted by biexponential function; thus, the lifetimes (τ_F(12T)) of the fast and slow components were evaluated to be 0.60 ps (fraction = 77%) and 10 ps (fraction = 23%), respectively. The fast fluorescence component is attributed to the energy redistribution via vibrational coupling,[17] because similar fast fluorescence decay was observed for the reference (12T) (0.56 ps; see the Supporting Information). The slow component is due to the $S_1 \rightarrow S_0$ transition, which is accelerated by the EN process from the ^{1}12T* moiety to the C_{60} moiety. Similar fluorescence decays were confirmed in the other triads, and the lifetimes are listed in Table 1. Although fast fluorescence lifetimes due of the energy redistribution via vibrational coupling are almost the same with length of *n*T, the slow fluorescence lifetimes of the triads increase with *n*T.

These longer τ_F values of the *n*T moieties in Fc-tm-*n*T-C_{60} are quite shorter than those of the $S_1 \rightarrow S_0$ transition for reference *n*T (τ_F(4T) = 390 ps, τ_F(8T) = 660 ps, and τ_F(12T) = 600 ps) in toluene (see the Supporting Information). The fluorescence quenching rate constants ($k_q(nT) = 1/\tau_F(nT)$) can be evaluated in the order of $10^{11}-10^{12}$ s^{-1} from the minor slow fluorescence decays of Fc-tm-*n*T-C_{60}; the k_q(*n*T) values decrease with the length of *n*T. The quantum yields ($\Phi_q(nT)$) for fluorescence quenching were evaluated to be almost unity. These

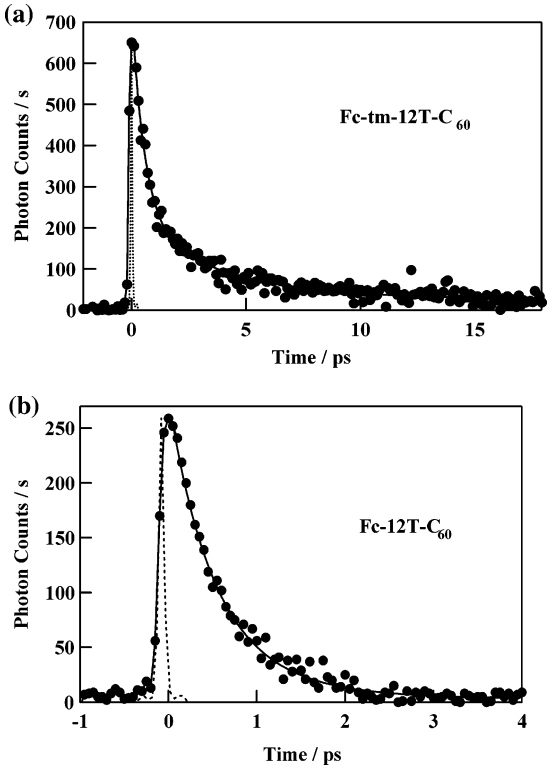

Figure 4. Time dependences of the fluorescence intensity for (a) Fc-tm-12T-C_{60} and (b) Fc-12T-C_{60} at 560 nm in toluene with 400-nm laser excitation; the dotted line indicates the laser profile.

TABLE 1: Fluorescence Lifetimes (τ_F) of *n*T and C_{60}

	In Toluene		In PhCN	
sample	τ_F(*n*T) (ps)	τ_F(C_{60}) (ps)	τ_F(*n*T) (ps)	τ_F(C_{60}) (ps)
Fc-tm-4T-C_{60}	0.34 (81%)	1300	0.38 (79%)	<10
Fc-tm-4T-C_{60}	0.74 (19%)	1300	0.69 (21%)	<10
Fc-tm-8T-C_{60}	0.64 (81%)	1300	0.67 (78%)	<10
Fc-tm-8T-C_{60}	7.4 (19%)	1300	7.4 (22%)	<10
Fc-tm-12T-C_{60}	0.60 (77%)	1300	0.61 (75%)	<10
Fc-tm-12T-C_{60}	10 (23%)	1300	9.1 (25%)	<10
Fc-4T-C_{60}	0.29 (75%)[a]	1300	0.27 (71%)[a]	<10
Fc-4T-C_{60}	0.58 (25%)[a]	1300	0.53 (29%)[a]	<10
Fc-8T-C_{60}	0.58 (77%)[a]	1300	0.51 (68%)[a]	<10
Fc-8T-C_{60}	1.5 (23%)[a]	1300	1.7 (32%)[a]	<10
Fc-12T-C_{60}	0.61 (68%)[a]	1300	0.53 (71%)[a]	<10
Fc-12T-C_{60}	2.3 (32%)[a]	1300	1.8 (29%)[a]	<10

[a] τ_F(Fc−*n*T).

k_q(*n*T) and Φ_q(*n*T) values can be predominantly attributed to the EN process to the C_{60} moiety in the triads (eq 1), because of the exothermic EN process in toluene.

$$\text{Fc-tm-}{}^1n\text{T*-C}_{60} \xrightarrow{k_{EN(T^*-C)}} \text{Fc-tm-}n\text{T-}{}^1\text{C}_{60}^* \qquad (1)$$

Figure 4b shows the time-dependent fluorescence intensity of the 12T moiety in Fc-12T-C_{60} in toluene. The fluorescence time profile of the ^{1}(Fc-12T)* moiety was also curve-fitted by biexponential function. The τ_F(Fc-*n*T) values for other ^{1}(Fc-*n*T)*-C_{60} are summarized in Table 1, in which the short τ_F(Fc-*n*T) can be attributed to the energy redistribution via vibrational coupling, whereas the long τ_F(Fc-*n*T) values can be attributed to the EN process from the ^{1}(Fc-*n*T)* moiety to the C_{60} moiety, as shown in eq 2, in which the excited singlet state of Fc-*n*T-C_{60} should be described as ^{1}(Fc-*n*T)*-C_{60}. As can be shown from the difference between Figures 4a and 4b for *n*T = 12T, the τ_F(Fc-*n*T) values of Fc-*n*T-C_{60} are smaller than those of Fc-tm-*n*T-C_{60}. The k_q(Fc-*n*T) values of Fc-*n*T-C_{60} can be calculated from the reciprocal of τ_F(Fc-*n*T), because the fluorescence lifetimes of the Fc-*n*T dyads are sufficiently longer than those of ^{1}(Fc-*n*T)*-C_{60}; the time profile of Fc-4T is shown in the Supporting Information as an example.

$$^1\text{(Fc-}n\text{T)*-C}_{60} \xrightarrow{k_{EN(FT^*-C)}} \text{Fc-}n\text{T-}{}^1\text{C}_{60}^* \qquad (2)$$

Similar fluorescence time profiles were observed for these triads in PhCN, from which the lifetimes were evaluated, as summarized in Table 1. The longer τ_F(*n*T) values of all these triads were almost equal to the corresponding ones in toluene, suggesting that the EN process predominantly occurs, even in polar PhCN. The $k_{EN(T^*-C)}$ and $k_{EN(FT^*-C)}$ values in PhCN are listed in Table 2, where exothermic EN processes are confirmed from negative ΔG_{EN} values.

On the basis of Förster theory,[18] the k_{EN} values for Fc-tm-*n*T-C_{60}were estimated to be 1.3×10^{12}, 1.1×10^{11}, and 0.98×10^{11} s^{-1} for *n*T = 4T, 8T, and 12, respectively, whereas those for Fc-*n*T-C_{60} were 2.2×10^{12}, 6.9×10^{11}, and 6.3×10^{11} s^{-1}, respectively. These values are in very good agreement with the experimentally obtained values in Table 2. The k_{EN} values for ^{1}(Fc-*n*T)*-C_{60} with broader fluorescence band are larger than those of Fc-tm-^{1}*n*T*-C_{60} except for *n*T = 4T (see the Supporting Information).

Fluorescence Dynamics of the C_{60} Moiety. To investigate the CS process from the $^1C_{60}$* moiety, the time-resolved fluorescence was measured using the streak scope with a time resolution of 10 ps, because the fluorescence bands due to the $^1C_{60}$* moiety appear out of the measurable region of our fluorescence upconversion system. The fluorescence lifetimes of the C_{60} moiety in Fc-tm-*n*T-C_{60} and Fc-*n*T-C_{60} are listed in Table 1. In toluene, the fluorescence lifetimes of the triads were evaluated to be 1.3 ns, which is equal to that of NMPC_{60}. Hence, no CS state was formed in toluene from the $^1C_{60}$* moiety. On the other hand, the fluorescence lifetimes of the $^1C_{60}$* moiety in PhCN were estimated to be <10 ps, indicating that the CS states were formed from Fc-tm-*n*T-$^1C_{60}$* (eq 3) with the quantum yield of almost unity. As the generation of the $^1C_{60}$* moiety in the triads, both direct excitation and indirect formation via the EN process from the ^1nT* moiety may be considered, depending on the excitation wavelength. The CS process via the $^1C_{60}$* moiety is thermodynamically possible in PhCN (Table 2).[19]

$$\text{Fc-tm-}n\text{T-}{}^1\text{C}_{60}^* \xrightarrow[k_{CS(T-C^*)}]{<10\text{ ps in PhCN}} \text{Fc-tm-}n\text{T}^{\bullet+}\text{-C}_{60}^{\bullet-} \qquad (3)$$

In the case of the CS state for Fc-*n*T-C_{60}, (Fc-*n*T)$^{\bullet+}$-$C_{60}^{\bullet-}$ may be generated after delocalization of the radical cation between the *n*T and Fc moieties via π-conjugation. The CS processes generating (Fc-*n*T)$^{\bullet+}$-$C_{60}^{\bullet-}$ via Fc-*n*T-$^1C_{60}$* are thermodynamically possible in PhCN (see Table 2). As described in the latter part of this paper, process 4, which generates (Fc-*n*T)$^{\bullet+}$-$C_{60}^{\bullet-}$, can be confirmed on the basis of the picosecond transient absorption spectra.

$$\text{Fc-}n\text{T-}{}^1\text{C}_{60}^* \xrightarrow[k_{CS(T-C^*)}]{<10\text{ ps in PhCN}} (\text{Fc-}n\text{T})^{\bullet+}\text{-C}_{60}^{\bullet-} \qquad (4)$$

Transient Absorption Study in Toluene. Figure 5a shows the transient absorption spectra of Fc-12T-C_{60} at 1.0 and 500 ps in toluene after laser irradiation, when the 12T moiety was mainly excited with 388-nm light. In Figure 5a, the absorption band due to the ^{1}12T* moiety appeared at ~890 nm at 1.0 ps.[20] Although the most of the absorption of the ^{1}12T* moiety at

TABLE 2: Driving Forces ($-\Delta G_{CS}$, $-\Delta G_{EN}$, and $-\Delta G_{HS}$) and Rate Constants ($k_{CS(T-C^*)}$, $k_{EN(T^*-C)}$, and $k_{HS(F\leftarrow T)}$) of Fc-tm-*n*T-C_{60} and Fc-*n*T-C_{60} in PhCN

			$n = 4$		$n = 8$		$n = 12$	
initial state	final state		$-\Delta G$ (eV)[a]	k (s^{-1})	$-\Delta G$ (eV)	k (s^{-1})	$-\Delta G$ (eV)	k (s^{-1})
Fc-tm-^1nT*-C_{60}	Fc-tm-*n*T-$^1C_{60}$*	$k_{EN(T^*-C)}$	0.61	1.4×10^{12}[b]	0.39	1.3×10^{11}[b]	0.33	1.1×10^{11}[b]
Fc-tm-*n*T-$^1C_{60}$*	Fc-tm-*n*T$^{\bullet+}$-$C_{60}^{\bullet-}$	$k_{CS(T-C^*)}$	0.34	8.1×10^{11}	0.44	4.5×10^{11}	0.57	2.8×10^{11}
Fc-tm-*n*T$^{\bullet+}$-$C_{60}^{\bullet-}$	Fc$^{\bullet+}$-tm-*n*T-$C_{60}^{\bullet-}$	$k_{HS(F\leftarrow T)}$	0.46[c]	3.8×10^{10}[d]	0.35[c]	3.1×10^{10}[d]	0.23[c]	1.3×10^{10}[d]
	Fc-tm-*n*T-C_{60}	$k_{CR(T-C)}$	1.42		1.32		1.11	
^{1}(Fc-*n*T)*-C_{60}	Fc-*n*T-$^1C_{60}$*	$k_{EN(FT^*-C)}$	0.71	1.9×10^{12}[b]	0.39	6.7×10^{11}[b]	0.32	5.6×10^{11}[b]
Fc-*n*T-$^1C_{60}$*	(Fc-*n*T)$^{\bullet+}$-$C_{60}^{\bullet-}$	$k_{CS(FT-C^*)}$	0.57	$>1.0 \times 10^{11}$	0.62	$>1.0 \times 10^{11}$	0.69	$>1.0 \times 10^{11}$

[a] ΔG_{CS} values in PhCN were calculated using the following Weller equations:[13] $-\Delta G_{CS} = \Delta E_{0-0} - (E_{ox} - E_{red} + \Delta G_S)$ and $-\Delta G_S = e^2/(4\pi\epsilon_0\epsilon_R R(D-A))$, where ΔE_{0-0} (Fc-tm-nT-C_{60}; 2.70 eV for 4T, 2.24 eV for 8T, 2.21 eV for 12T, and 1.70 eV for $^1C_{60}$* and Fc-nT-C_{60}; 2.41 eV for 4T, 2.09 eV for 8T, and 2.02 eV for 12T), E_{ox} and E_{red} are the oxidation potentials of the *n*T moiety and reduction potential of the C_{60} moiety in the triads,[13] and ΔG_S is a static Coulomb interaction, in which ϵ_0 and ϵ_R refer to the vacuum permittivity and dielectric constant of PhCN, respectively, and R(D−A) to center-to-center distance of the *n*T and C_{60} moieties evaluated by the molecular orbital calculations. In Fc-tm-*n*T-C_{60}, R(Fc-C_{60}) = 22.8, 35.7, and 50.9 Å, and R(*n*T-C_{60}) = 12.8, 20.4, and 27.9 Å for $n = 4$, 8 and 12, respectively. In Fc-*n*T-C_{60}, R(Fc-C_{60}) = 22.5, 35.4, and 50.5 Å, and R(*n*T-C_{60}) = 12.8, 20.4, and 27.9 Å for $n = 4$, 8, and 12, respectively. ΔG_{CS} values in toluene calculated are all positive. [b] From slow fluorescence decay; $k_{EN(T^*-C)} = (\tau_F)^{-1} - (\tau_0)^{-1}$. [c] $-\Delta G_{HS(F\leftarrow T)} = -\Delta G_{CR(T-C)} - (-\Delta G_{CR(F-C)})$; $\Delta G_{CR} = E_{ox} - E_{red} + \Delta G_S$. [d] Sum of the CR rate from Fc-tm-*n*T$^{\bullet+}$-$C_{60}^{\bullet-}$ to Fc-tm-*n*T-C_{60} and the HS rate from Fc-tm-*n*T$^{\bullet+}$-$C_{60}^{\bullet-}$ to Fc$^{\bullet+}$-tm-*n*T-$C_{60}^{\bullet-}$.

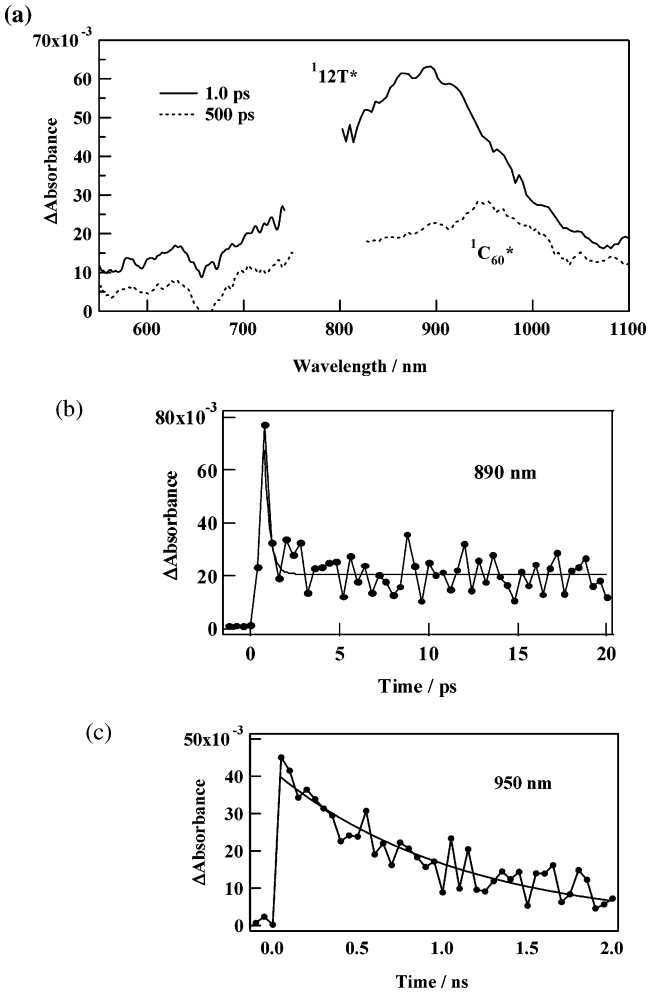

Figure 5. (a) Transient absorption spectra of Fc-12T-C_{60} in toluene at 1.0 and 500 ps after 388-nm laser irradiation. (b and c) Absorption temporal profiles at 890 and 950 nm, respectively.

890 nm decayed rapidly until 2.0 ps (Figure 5b), the absorption of the $^1C_{60}$* moiety remained at 950 nm,[20] as shown in the spectrum at 500 ps. This finding suggests that the EN process predominantly occurs from the ^{1}12T* moiety to the C_{60} moiety in toluene. The temporal profile at 950 nm until 2 ns is shown in Figure 5c. The decay profile was best curve-fitted with a single-exponential function, giving the time constant to be 1.1 ns, which is in good agreement with the fluorescence lifetime of the $^1C_{60}$* moiety in toluene (1.3 ns). Thus, no CS state was formed from Fc-12T-$^1C_{60}$*. The slow decay part at 890 nm in Figure 5b is expected to be the absorption tail of Fc-12T-$^1C_{60}$*. Similar findings were also confirmed in other triads (Fc-tm-*n*T-C_{60} and Fc-*n*T-C_{60}).

Charge Separation and Hole Shift of Fc-tm-*n*T-C_{60} in PhCN by Picosecond Transient Absorption Study. Figure 6a depicts the transient absorption spectra of Fc-tm-12T-C_{60} at 1.0, 3.0, and 1800 ps in PhCN after laser irradiation (150 fs, 388 nm). The absorption band of the ^{1}12T* moiety was confirmed at ~900 nm at 1.0 ps. At 3.0 ps, the absorption bands appearing at 820 and 1050 nm are attributed to the 12T$^{\bullet+}$ moiety and the $C_{60}^{\bullet-}$ moiety, respectively. This finding indicates the formation of Fc-tm-12T$^{\bullet+}$-$C_{60}^{\bullet-}$. After 1800 ps, the absorption band of the 12T$^{\bullet+}$ moiety decayed, while the absorption of the $C_{60}^{\bullet-}$ moiety remained. Hence, the hole shift from the 12T$^{\bullet+}$ moiety to the Fc moiety occurs competitively with vicinal charge recombination between the 12T$^{\bullet+}$ moiety and the $C_{60}^{\bullet-}$ moiety; i.e., the remaining fraction of the $C_{60}^{\bullet-}$ moiety at 1800 ps can be thought as a counterpart of the Fc$^{\bullet+}$ moiety of Fc$^{\bullet+}$-tm-12T-$C_{60}^{\bullet-}$.

The short-time scale temporal profile at 850 nm in inset of Figure 6b should be analyzed using a three-exponential function; i.e., the fast and slow decay components of the ^{1}12T* moiety and the slow rise of the 12T$^{\bullet+}$ moiety. The time constant for this rise of the 12T$^{\bullet+}$ moiety was evaluated to be 3.6 ps ($= (k_{CS(T-C^*)})^{-1}$) from the best-fitted curve. In this analysis, the time constants of the fast and slow decay of the ^{1}12T* moiety were fixed at 0.61 and 9.1 ps, which were cited from the time-resolved fluorescence lifetimes in PhCN. The absorption rise of the 12T$^{\bullet+}$ moiety suggests that Fc-tm-12T$^{\bullet+}$-$C_{60}^{\bullet-}$ was formed via Fc-tm-12T-$^1C_{60}$* after the EN process from Fc-tm-^{1}12T*-C_{60} ($k_{EN(T^*-C)} = 1.1 \times 10^{11}$ s^{-1}). The observation of the absorption rise of the $^1C_{60}$* moiety was impossible, because the rate for the CS process from Fc-tm-12T-$^1C_{60}$* ($k_{CS(T-C^*)} = 2.8 \times 10^{11}$ s^{-1}) is faster than that for the EN process. For the other Fc-tm-*n*T-C_{60}, the $k_{CS(T^*-C)}$ values were similarly evaluated (see Table 2).

In the long time-scale measurement (Figure 6b), the temporal profile of the 12T$^{\bullet+}$ moiety at 850 nm shows fast and slow decay. The fast decay includes two pathways: the positive charge-shift process from the 12T$^{\bullet+}$ moiety to the Fc moiety (eq 5) and the CR process between the 12T$^{\bullet+}$ and $C_{60}^{\bullet-}$ moieties (eq 6). The rate constant for the fast decay was evaluated to be 1.5×10^{10} s^{-1} from the best-fitted curve to the temporal profile at 850 nm (Figure 6b), and this rate constant is the sum of the

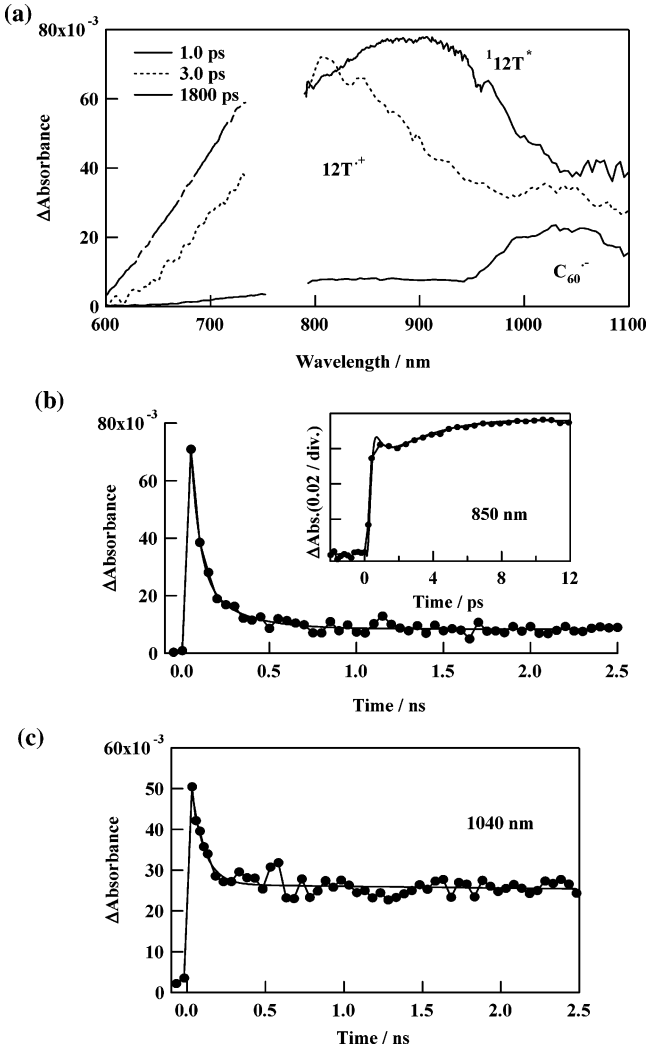

Figure 6. (a): Transient absorption spectra of Fc-tm-12T-C_{60} in PhCN at 1.0, 3.0, and 1800 ps after 388-nm laser irradiation. (b and c) Absorption temporal profiles at 850 and 1040 nm, respectively.

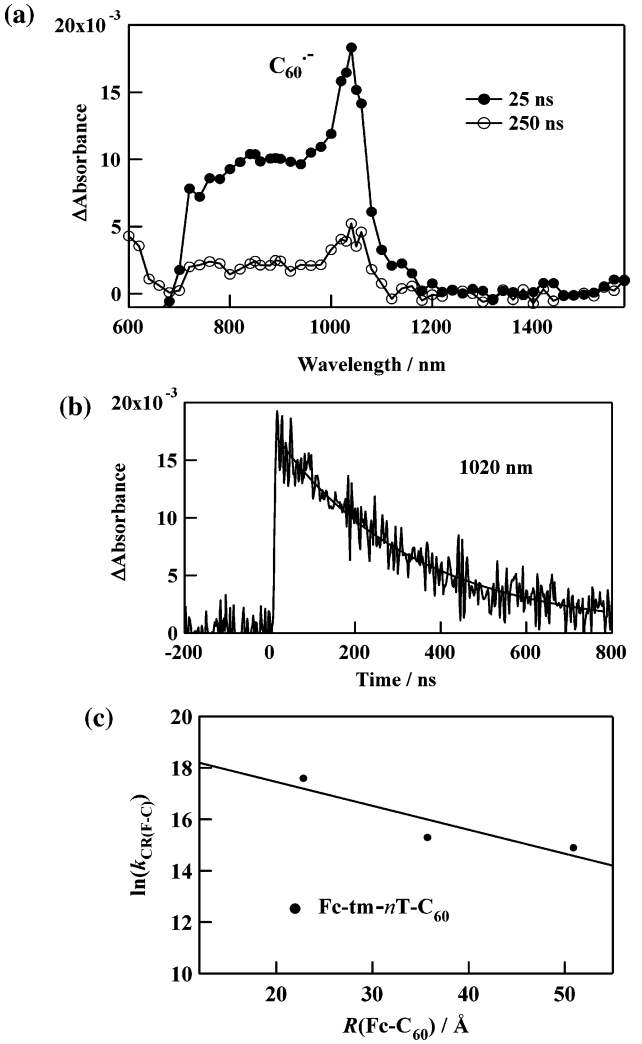

Figure 7. (a) Transient absorption spectra of Fc-tm-12T-C_{60} in PhCN at 25 ns and 250 ns after 532-nm laser irradiation. (b) Absorption temporal profile at 1020 nm. (c) Distance (R(Fc-C_{60})) dependence of the CR rate constants. The line represents the best fit to eq 8.

CR rate between the 12T$^{\bullet+}$ moiety and the $C_{60}^{\bullet-}$ moiety ($k_{CR(T-C)}$) and the hole-shift rate ($k_{HS(F\leftarrow T)}$) from the 12T$^{\bullet+}$ moiety to the Fc moiety.

Fast decay was also observed in the temporal profile at 1040 nm, as shown in Figure 6c; the decay may contain both the decay of the $C_{60}^{\bullet-}$ moiety and the 12T$^{\bullet+}$ moiety, because the absorption tail of the 12T$^{\bullet+}$ moiety may be overlapped with the absorption of the $C_{60}^{\bullet-}$ moiety at 1040 nm. Therefore, the $k_{CR(T-C)}$ value could not be separately evaluated from the $k_{HS(F\leftarrow T)}$ value; thus, the sum of them are listed in Table 2.

$$\text{Fc-tm-}n\text{T}^{\bullet+}\text{-C}_{60}^{\bullet-} \xrightarrow{k_{HS(F\leftarrow T)}} \text{Fc}^{\bullet+}\text{-tm-}n\text{T-C}_{60}^{\bullet-} \quad (5)$$

$$\text{Fc-tm-}n\text{T}^{\bullet+}\text{-C}_{60}^{\bullet-} \xrightarrow{k_{CR(T-C)}} \text{Fc-tm-}n\text{T-C}_{60} \quad (6)$$

Charge-Recombination Process of Fc-tm-*n*T-C_{60} by Nanosecond Transient Study. The nanosecond transient absorption spectra of Fc-tm-12T-C_{60} were observed with the 532-nm laser irradiation in PhCN, as shown in Figure 7a. The absorption band observed around 1020 nm with the shoulder in the range of 700−950 nm was attributed to the $C_{60}^{\bullet-}$ moiety, suggesting the formation of Fc$^{\bullet+}$-tm-12T-$C_{60}^{\bullet-}$, because the absorption shape was similar to that observed at 1800 ps in Figure 6a. The absence of the near-IR broad band characteristic of 12T$^{\bullet+}$ in the region of 1200−1600 nm (see the Supporting Information) also supports the generation of Fc$^{\bullet+}$-tm-12T-$C_{60}^{\bullet-}$ in the nanosecond time regions. From the temporal profile of the $C_{60}^{\bullet-}$ moiety at 1020 nm in Figure 7b, the decay rate of Fc$^{\bullet+}$-tm-12T-$C_{60}^{\bullet-}$ was estimated to be 3.0×10^7 s^{-1}. Similar findings were confirmed in the other Fc-tm-*n*T-C_{60} and the CR rate constants ($k_{CR(F-C)}$) are summarized in Table 3. These $k_{CR(F-C)}$ values decrease with the length of the *n*T moiety. If the stepwise charge recombination occurs, the barriers for the hole hopping from the Fc moiety (E_{ox}(Fc) = 0.40 V vs Ag/Ag$^+$) to the *n*T moiety decreased in the order of oxidation potentials of the *n*T moieties; (E_{ox}(4T)

TABLE 3: Driving Forces of CR ($-\Delta G_{CR}$) and Rate Constants (k_{CR}) for CR and Lifetimes of Radical Ion-Pair (τ_{RIP}) of Fc-tm-*n*T-C_{60} and Fc-*n*T-C_{60} in PhCN

initial state	final state	$-\Delta G_{CR}$ (eV)[a]	k_{CR} (s^{-1})[b]	τ_{RIP} (ns)
Fc$^{\bullet+}$-tm-4T-C$_{60}^{\bullet-}$	Fc-tm-4T-C_{60}	0.96	4.6×10^7	22
Fc$^{\bullet+}$-tm-8T-C$_{60}^{\bullet-}$	Fc-tm-8T-C_{60}	0.97	4.2×10^6	240
Fc$^{\bullet+}$-tm-12T-C$_{60}^{\bullet-}$	Fc-tm-12T-C_{60}	0.98	3.0×10^6	330
(Fc-4T)$^{\bullet+}$-C$_{60}^{\bullet-}$	Fc-4T-C_{60}	1.52	1.2×10^{10}	0.083
(Fc-8T)$^{\bullet+}$-C$_{60}^{\bullet-}$	Fc-8T-C_{60}	1.32	3.7×10^8	2.7
(Fc-12T)$^{\bullet+}$-C$_{60}^{\bullet-}$	Fc-12T-C_{60}	1.20	2.0×10^7	50

[a] See footnote in Table 2. [b] $k_{CR(F-C)}$ for Fc-tm-*n*T-C_{60} and $k_{CR(FT-C)}$ for Fc-*n*T-C_{60}.

= 0.87 V) > (E_{ox}(8T) = 0.76 V) > (E_{ox}(12T) = 0.64 V) vs Ag/Ag$^+$.[16] These E_{ox}(nT) values predict the opposite tendency to the observed $k_{CR(F-C)}$ values. Therefore, the CR process happens directly between the Fc$^{\bullet+}$ moiety and the $C_{60}^{\bullet-}$ moiety via the nT moiety, as shown in eq 7, in which the nT moieties act as molecular spacers:

$$Fc^{\bullet+}\text{-tm-}n\text{T-}C_{60}^{\bullet-} \xrightarrow{k_{CR(F-C)}} \text{Fc-tm-}n\text{T-}C_{60} \quad (7)$$

Figure 7c depicts the plots of ln($k_{CR(F-C)}$) vs R(Fc-C_{60}) for Fc-tm-nT-C_{60} in PhCN, in which the R(Fc-C_{60}) values were evaluated from the optimized structures (see margin of Table 2). The attenuation factor (β), which reflects the nature of the bridge molecules, can be evaluated from eq 8:[21]

$$\ln(k_{CR(F-C)}) = \ln k_0 - \beta R(\text{Fc-}C_{60}) \quad (8)$$

From the slope of Figure 7c, the β value for $k_{CR(F-C)}$ of Fc-tm-nT-C_{60} in PhCN was estimated to be 0.10 Å^{-1}, which is much smaller than the reported β values for charge-recombination processes.[21]

Transient Absorption Study on Fc-nT-C_{60} in PhCN. Using the 150-fs laser excitation (388 nm) of the 12T moiety of Fc-12T-C_{60} in PhCN, the transient absorption bands appeared at 820 and 1040 nm at 500 ps after the rapid decay of the ^{1}12T* moiety at ~900 nm, as shown in Figure 8a. The 820-nm band was due to the 12T$^{\bullet+}$ moiety,[20] whereas the 1040-nm band was attributed to be the $C_{60}^{\bullet-}$ moiety.[22] For reference compounds, the extinction coefficients of 12T$^{\bullet+}$ and NMP$C_{60}^{\bullet-}$ were reported to be (ϵ(12T$^{\bullet+}$)$_{820\,nm}$ ≈ 32 000 M^{-1} cm^{-1} and ϵ(NMP$C_{60}^{\bullet-}$)$_{1040\,nm}$ = 7000 M^{-1} cm^{-1});[22] one example was shown in the transient absorption spectrum at 3.0 ps in Figure 6a for Fc-tm-12T$^{\bullet+}$-$C_{60}^{\bullet-}$. However, the observed ratio of the absorbance at 820 nm (mainly of the 12T$^{\bullet+}$ moiety) to that at 1040 nm of the $C_{60}^{\bullet-}$ moiety at 500 ps was almost $^1/_2$ in Figure 8a. Therefore, it can be presumed that most of the radical cation of the 12T$^{\bullet+}$ moiety delocalized to the Fc moiety, generating (Fc-12T)$^{\bullet+}$-$C_{60}^{\bullet-}$, because Fc$^{\bullet+}$ has no appreciable absorption intensity in these wavelength regions. Thus, it was revealed that the directly linked Fc-12T moiety behaves as one donor for the C_{60} moiety. In a 500-ps spectrum, it was difficult to observe the absorption of the $^1C_{60}$* moiety, because the fluorescence of the $^1C_{60}$* moiety decayed within 10 ps, generating (Fc-12T)$^{\bullet+}$-$C_{60}^{\bullet-}$.

Figures 8b and 8c exhibit the temporal profiles at 820 nm (for (Fc-12T)$^{\bullet+}$) and 1040 nm (for the $C_{60}^{\bullet-}$ moiety), in which the slow decay parts are seen after initial rapid decay within 2 ps. The fast decay is attributed to the decay of ^{1}12T*. From the slow decay parts, the rate constant of the CR process from (Fc-12T)$^{\bullet+}$-$C_{60}^{\bullet-}$ to Fc-12T-C_{60} (eq 9) was estimated to be 2.0 × 10^7 s^{-1}, corresponding to the lifetimes (τ_{RIP} = 50 ns) of (Fc-12T)$^{\bullet+}$-$C_{60}^{\bullet-}$. Similar CS states were confirmed in Fc-4T-C_{60} and Fc-8T-C_{60}, but the CR process occurred within a few nanoseconds, as listed in Table 3.

$$(\text{Fc-}n\text{T})^{\bullet+}\text{-}C_{60}^{\bullet-} \xrightarrow{k_{CR(FT-C)}} \text{Fc-}n\text{T-}C_{60} \quad (9)$$

Figure 9a shows the nanosecond absorption spectra of Fc-12T-C_{60} at 25 ns in PhCN after 532-nm laser irradiation, which mainly excited the 12T moiety (>90%). The spectrum at 25 ns shows the absorption peak of the $C_{60}^{\bullet-}$ moiety at 1000 nm; in addition, the absorption bands of the 12T$^{\bullet+}$ moiety appeared in the 600−900 nm region as a shoulder and broad bands in the entire region of 1100−1600 nm. Compared with

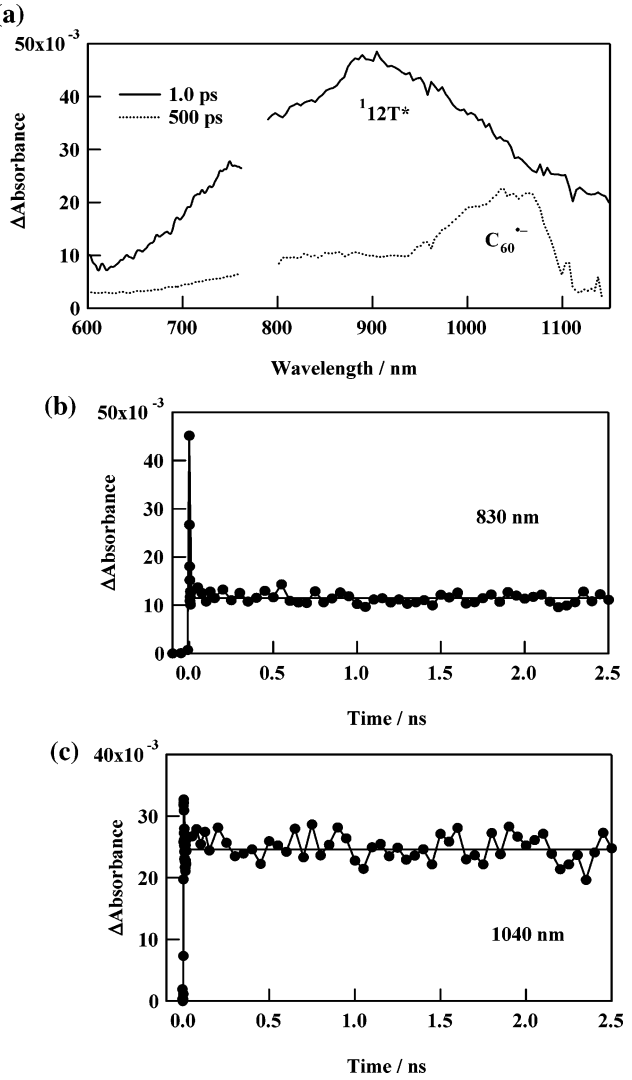

Figure 8. (a) Transient absorption spectra of Fc-12T−C_{60} in PhCN at 1.0 and 500 ps after 388-nm laser irradiation. (b and c) Absorption temporal profile at 830 and 1040 nm, respectively.

the absorption bands of 12T$^{\bullet+}$, which shows clear peaks at 840 nm and <1300 nm (see Figure S2 in the Supporting Information), the absorption of the 12T$^{\bullet+}$ moiety in Fc-12T-C_{60} is broad, as shown in Figure 9a. In addition, the absorption intensity ratio of 12T$^{\bullet+}$ to $C_{60}^{\bullet-}$ does not also obey the relation of the extinction coefficients (ϵ(12T$^{\bullet+}$)$_{820\,nm}$ > ϵ(NMP$C_{60}^{\bullet-}$)$_{1040\,nm}$).[20,22] These observations support the generation of (Fc-12T)$^{\bullet+}$-$C_{60}^{\bullet-}$. A similar finding was confirmed for Fc-8T-C_{60}; for Fc-4T-C_{60}, however, this behavior was not observed, because the CR process occurred with 1 ns.

The decay rate of the broad absorption at 1500 nm, (Figure 9c), which can be attributed to the (Fc-12T)$^{\bullet+}$ moiety, was estimated to be 2.0 × 10^7 s^{-1}. This value is equal to that of the $C_{60}^{\bullet-}$ moiety (Figure 9b); therefore, this rate constant can be attributed to the CR process from (Fc-12T)$^{\bullet+}$-$C_{60}^{\bullet-}$ to Fc-12T-C_{60} (eq 9), as summarized in Table 3.

Energy Diagram and Comparison of Two Types of Triads. Schematic energy diagrams of Fc-tm-nT-C_{60} and Fc-nT-C_{60} are shown in Figures 10a and 10b, respectively. In Fc-tm-nT-C_{60}, the downhill EN process occurred from the ^1nT* moiety to the C_{60} moiety after the energy redistribution of nT. After the EN process, the exothermic CS process occurs, generating Fc-tm-nT$^{\bullet+}$-$C_{60}^{\bullet-}$ within 10 ps. Then, the positive charge-shift process

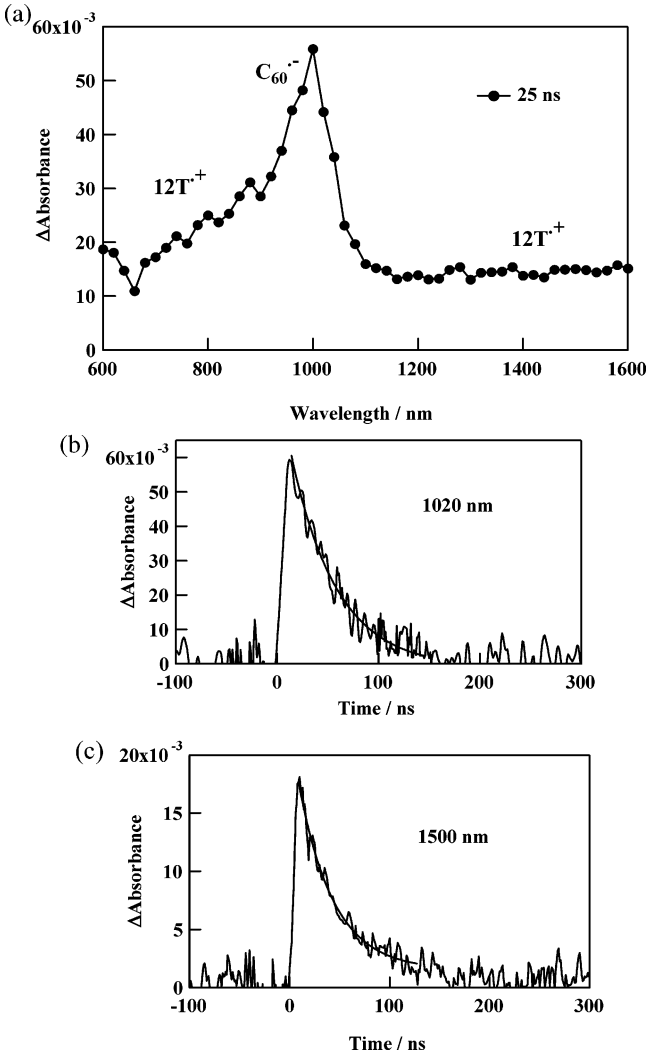

Figure 9. (a) Transient absorption spectrum of Fc-12T-C_{60} at 25 ns in PhCN after 532-nm laser irradiation. (b and c) Absorption temporal profiles at 1020 and 1500 nm, respectively.

from the nT$^{\bullet+}$ moiety to the Fc moiety occurs competing with the CR process of Fc-tm-nT$^{\bullet+}$-$C_{60}^{\bullet-}$ to the ground state.

In Fc-nT-C_{60} (Figure 10b), the energy level of (Fc-nT)$^{\bullet+}$-$C_{60}^{\bullet-}$ can be calculated from the average of the E_{ox} values of the nT and Fc moieties; thus, the energy level of (Fc-nT)$^{\bullet+}$-$C_{60}^{\bullet-}$ positioned between Fc-nT$^{\bullet+}$-$C_{60}^{\bullet-}$ and Fc$^{\bullet+}$-nT-$C_{60}^{\bullet-}$. The lifetime for the final CS state of Fc-tm-4T-C_{60} was longer than that of Fc-4T-C_{60}, by a factor of ~260; for nT = 8T and 12T, this factor is ~6−11. Hence, it was revealed that cutting π-conjugation was more effective for lasting the CS state than the charge delocalization between the nT and Fc moieties.

Comparison with Related Molecules. The damping factor (β) for ($k_{CR(F-C)}$) of Fc-tm-nT-C_{60} was estimated to be 0.10 Å^{-1} in PhCN. In the case of porphyrin-nT-C_{60}, in which the porphyrin moiety and the nT moiety are directly connected, the β value of nT for the CS rate constants was estimated to be 0.03 Å^{-1} in PhCN in our previous paper.[14a] Therefore, the large β value for Fc-tm-nT-C_{60} indicates that the methylene chain prevents the π-conjugation between the Fc and nT moieties.

The CR rates of the π-conjugation extended types (Fc-nT-C_{60}) were faster than those of nT-C_{60}.[12] In the cases of nT-C_{60}, the equilibrium exists between the CS state (nT$^{\bullet+}$-$C_{60}^{\bullet-}$) and the triplet state, which realizes the longer lifetime of the CS state, depending on the energy difference between the CS state and the triplet state. On the other hand, in Fc-nT-C_{60}, the lifetime

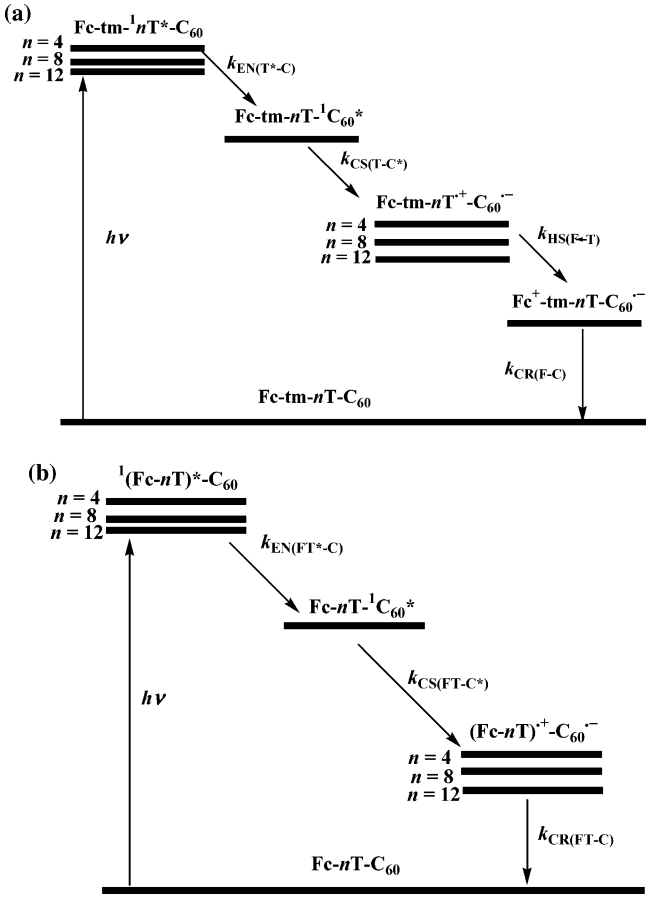

Figure 10. Schematic energy diagrams of (a) Fc-tm-nT-C_{60} and (b) Fc-nT-C_{60} in PhCN.

of the CS state obeys the energy difference between the CS state and the ground state, because the cation-radical delocalization stabilizes the CS state more than the triplet state.

Conclusion

Irrespective to the existence of methylene chain, the EN process occurred from the ^1nT* moiety to the C_{60} moiety at first, and then the CS process occurred via the $^1C_{60}$* moiety. Although the (Fc-nT) moiety in Fc-nT-C_{60} acts as a donor, three moieties in Fc-tm-nT-C_{60} work independently; especially, the hole shift from Fc-tm-nT$^{\bullet+}$-$C_{60}^{\bullet-}$ and Fc$^{\bullet+}$-tm-nT-$C_{60}^{\bullet-}$ was revealed. The prevention of π-conjugation between the Fc and nT moieties is more effective for maintaining the lifetime of the CS state than the positive-charge delocalization between the Fc and nT moieties by extending π-conjugation.

Acknowledgment. The present work was partly supported by a Grant-in-Aid for Scientific Research in Primary Area (417) from the Japan Society for the Promotion of Science and the Ministry of Education, Science, Sports and Culture of Japan.

Supporting Information Available: Optimized structures of Fc-tm-12T-C_{60} and Fc-12T-C_{60}, absorption spectrum of 12T$^{\bullet+}$, fluorescence time profiles of 12T and Fc-4T, transient absorption spectra and time profiles of Fc-12T-C_{60}, and absorption and fluorescence overlaps. This material is available free of charge via the Internet at http://pubs.acs.org.

References and Notes

(1) (a) Mitschke, U.; Bäuerle, P. *J. Mater. Chem.* **2000**, *10*, 1471. (b) Shirota, Y. *J. Mater. Chem.* **2000**, *10*, 1.

(2) (a) Harrison, M. G.; Friend R. H. In *Electronic Materials: The Oligomer Approach*; Müllen, K., Wegner, G., Eds.; Wiley−VCH: Weinheim, Germany, 1998; pp 515−558. (b) van Duren, J. K. J.; Dhanabalan, A.; van Hal, P. A.; Janssen, R. A. J. *Synth. Met.* **2001**, *121*, 1587.

(3) (a) Horowitz, G. *Adv. Mater*. **1998**, *10*, 365. (b) Dimitrakopoulos, C. D.; Malenfant, P. R. M. *Adv. Mater.* **2002**, *14*, 99.

(4) Nalwa, H. S. In *Handbook of Organic Conductive Molecules and Polymers*, Vol. 4; Nalwa, H. S., Ed.; Wiley: Chichester, U.K., 1997; pp 261−363.

(5) (a) Nakanishi, H.; Sumi, N.; Aso, Y.; Otsubo, T. *J. Org. Chem.* **1988**, *53*, 8632. (b) Nakanishi, H.; Aso, Y.; Otsubo, T. *Synth. Met.* **1999**, *101*, 413. (c) Nakanishi, H.; Sumi, N.; Ueno, S.; Takimiya, K.; Aso, Y.; Otsubo, T.; Komaguchi, K.; Shiotani, M.; Ohta, N. *Synth. Met*. **2001**, *119*, 413.

(6) (a) Otsubo, T.; Aso, Y.; Takimiya, K. *Bull. Chem. Soc. Jpn.* **2001**, *74*, 1789. (b) Otsubo, T.; Aso, Y.; Takimiya, K. *J. Mater. Chem.* **2002**, *12*, 2565.

(7) (a) Roncali, J. *Chem. Rev.* **1992**, *92*, 711. (b) Smith, J. R.; Cox, P. A.; Campbell, S. A.; Ratcliffe, N. M. *J. Chem. Soc., Faraday Trans.* **1995**, *91*, 2331. (c) Apperloo, J. J.; Janssen, R. A. J.; Malenfant, P. R. L.; Fréchet, J. M. J. *J. Am. Chem. Soc.* **2001**, *123*, 6919.

(8) (a) Segawa, H.; Wu, F.-P.; Nakayama, N.; Maruyama, H.; Sagisaka, S.; Higuchi, N.; Fujitsuka, M.; Shimidzu, T. *Synth. Met.* **1995**, *71*, 2151. (b) Fujitsuka, M.; Sato, T.; Segawa, H.; Simidzu, T. *Synth. Met.* **1995**, *69*, 309.

(9) (a) Kroto, H. W.; Heath, J. R.; O'Brien, S, C.; Curl, R. F.; Smalley, R. E. *Nature* **1985**, *318*, 162. (b) Haddon, R. C. *Acc. Chem. Res.* **1988**, *21*, 243. (c) Haddon, R. C. *Science* **1993**, *261*, 1545. (d) Sassara, A.; Zerza, G.; Chergui, M. *J. Phys. B* **1996**, *29*, 4997. (e) Negri, F.; Orlandi, G.; Zerebetto, F. *J. Phys. Chem.* **1996**, *100*, 10849. (f) Dauw, X. L. R.; Bronsveld, M. V.; Krüger, A.; Warntjes, J. B. M.; Witjes, M. R. *J. Chem. Phys.* **1998**, *109*, 21.

(10) (a) Imahori, H.; Cardoso, S.; Tatman, D.; Lin, S.; Noss, L.; Seely, G. R.; Sereno, L.; Silber, C.; Moore, T. A.; Moore, A. L.; Gust, D. *J. Photochem. Photobiol. A* **1995**, *62*, 1009. (b) Imahori, H.; Hagiwara, K.; Akiyama, T.; Aoki, M.; Taniguchi, S.; Okada, T.; Shirakawa, M.; Sakata, Y. *Chem. Phys. Lett.* **1996**, *263*, 545. (c) Guldi, D. M.; Garscia, G. T.; Mattay, J. *J. Phys. Chem. A* **1998**, *102*, 9679. (d) Tkachenko, N. V.; Rantala, L.; Tauber, A. Y.; Helaja, J.; Hynninen, P. V.; Lemmetyinen, H. *J. Am. Chem. Soc.* **1999**, *121*, 9378. (e) van Hal, P. A.; Knol, J.; Langeveld-Voss, B. M. W.; Meskers, S. C. J.; Hummelen, J. C.; Janssen, R. A. J. *J. Phys. Chem. A* **2000**, *104*, 5974. (f) Apperloo, J. J.; Langeveld-Voss, B. M. W.; Knol, J.; Hummelen, J. C.; Janssen, R. A. J. *Adv. Mater.* **2000**, *12*, 908. (g) van Hal, P. A.; Beckers, E. H. A.; Meskers, S. C. J.; Janssen, R. A. J.; Jousselme, B.; Blanchard, P.; Roncali, J. *Chem.−Eur. J.* **2002**, *8*, 5415. (h) Beckers, E. H. A.; van Hal, P. A.; Dhanabalan, A.; Meskers, S. C. J.; Knol, J.; Hummelen, J. C.; Janssen, R. A. J. *J. Phys. Chem. A* **2003**, *107*, 6218.

(11) Matsumoto, K.; Fujitsuka, M.; Sato, T.; Onodera, S.; Ito, O. *J. Phys. Chem. B* **2000**, *104*, 11632.

(12) (a) Yamashiro, T.; Aso, Y.; Otsubo, T.; Tang, H.; Harima, Y.; Yamashita, K. *Chem. Lett.* **1999**, *28*, 443. (b) Fujitsuka, M.; Ito, O.; Yamashiro, T.; Aso, Y.; Otsubo, T. *J. Phys. Chem. A* **2000**, *104*, 4876. (c) Fujitsuka, M.; Matsumoto, K.; Ito, O.; Yamashiro, T.; Aso, Y.; Otsubo, T. *Res. Chem. Intermed.* **2001**, *27*, 73. (d) Fujitsuka, M.; Masuhara, A.; Kasai, H.; Oikawa, H.; Nakanishi, H.; Ito, O.; Yamashiro, T.; Aso, Y.; Otsubo, T. *J. Phys. Chem. B* **2001**, *105*, 9930.

(13) (a) Marcus, R. A. *J. Chem. Phys.* **1956**, *24*, 966. (b) Marcus, R. A. *J. Chem. Phys.* **1957**, *26*, 867. (c) Marcus, R. A. *J. Chem. Phys.* **1957**, *26*, 872. (d) Marcus, R. A. *J. Chem. Phys.* **1965**, *43*, 679. (e) Marcus, R. A.; Sutin, N. *Biochim. Biophys. Acta* **1985**, *811*, 265.

(14) (a) Nakamura, T.; Fujitsuka, M.; Araki, Y.; Ito, O.; Ikemoto, J.; Takimiya, K.; Aso, Y.; Otsubo, T. *J. Phys. Chem. B* **2004**, *108*, 10700. (b) Nakamura, T.; Ikemoto, J.; Fujitsuka, M.; Araki, Y.; Ito, O.; Takimiya, K.; Aso, Y.; Otsubo, T. *J. Phys. Chem. B* **2005**, *109*, 14365.

(15) (a) Luo, C.-P.; Guldi, D. M.; Imahori, H.; Tamaki, K.; Sakata, Y. *J. Am. Chem. Soc*. **2000**, *122*, 6535. (b) Fukuzumi, S.; Imahori, H.; Yamada, H.; El-Khouly, M. E.; Fujitsuka, M.; Ito, O.; Guldi, D. M. *J. Am. Chem. Soc*. **2001**, *123*, 2571. (c) Imahori, H.; Tamaki, K.; Guldi, D. M.; Luo. C.-P.; Fujitsuka, M.; Ito, O.; Fukuzumi, S. *J. Am. Chem. Soc*. **2001**, *123*, 2607. (d) Imahori, H.; Guldi, D. M.; Tamaki, K.; Yoshida, Y.; Luo, C.-P.; Sakata, Y.; Fukuzumi, S. *J. Am. Chem. Soc*. **2001,** *123*, 6617. (e) Imahori, H.; Tamaki, K.; Araki, Y.; Sekiguchi, Y.; Ito, O.; Sakata, Y.; Fukuzumi, S. *J. Am. Chem. Soc.* **2002**, *124*, 5165.

(16) Kanato, H.; Takimiya, K.; Otsubo, T.; Aso, Y.; Nakamura, T.; Araki, Y.; Ito, O. *J. Org. Chem.* **2004**, *69*, 7183.

(17) (a) Lanzani, G.; Nisoli, M.; Magni, V.; De Silvestri, S.; Barbarella, G.; Zambianchi, M.; Tubino, R. *Phys. Rev. B* **1995**, *51*, 13770. (b) Lanzani, G.; Nisoli, N.; De Silvestri, S.; Tubino, R. *Chem. Phys. Lett.* **1996**, *251*, 339. (c) Wong, K. S.; Wang, H.; Lanzani, G. *Chem. Phys. Lett.* **1998**, *288*, 59. (d) Lanzani, G.; Cerullo, G.; Stagira, S.; De Silvestri, S. *J. Photochem. Photobiol. A* **2001**, *144*, 13.

(18) (a) Förster, T. *Ann. Phys.* **1948**, *2*, 55. (b) Calvert, J. G.; Pitts, J. N., Jr. *Photochemistry*; Wiley: New York, 1967; pp 339−365.

(19) (a) Weller, A. *Z. Phys. Chem.* **1982**, *132*, 93. (b) Gaines, G. L.; O'Neil, M. P.; Svec, W. A.; Niemczyk, M. P.; Wasielewski, M. R. *J. Am. Chem. Soc.* **1991**, *113*, 719.

(20) (a) Becker, R. S.; de Melo, J. S.; Maçantia, A. L.; Elisei, F. *Pure. Appl. Chem.* **1995**, *67*, 9 (b) Becker, R. S.; de Melo, J. S.; Maçantia, A. L.; Elisei, F. *J. Phys. Chem.* **1996**, *100*, 1863. (c) de Melo, J. S.; Silva, L. M.; Arnaut, L. G.; Becker, R. S. *J. Chem. Phys.* **1999**, *12*, 5427.

(21) (a) Marcus, R. A.; Sutin, N. *Biochim. Biophys. Acta* **1985**, *811*, 265. (b) Levich, V. G. *Adv. Electrochem. Eng*. **1966**, *4*, 249. (c) Jornter, J. *J. Chem. Phys.* **1976**, *64*, 4860. (d) Bixon, M.; Jornter, J. *Adv. Chem. Phys.* **1999**, *106*, 35. (e) Lokan, N. R.; Paddon-Row: M. N.; Koeberg; M.; Verhoeven, J. W. *J. Am. Chem. Soc.* **2000**, *122*, 5075. (f) Kang, Y. K.; Rubtsov, I. V.; Iovine, P. M.; Chen, J.; Therien, M. J. *J. Am. Chem. Soc.* **2002**, *124*, 8275.

(22) (a) Luo, C.-P.; Fujitsuka, M.; Watanabe, A.; Ito, O.; Gan, L.; Huang, Y.; Huang, C.-H. *J. Chem. Soc., Faraday Trans.* **1998**, *84*, 527. (b) Guldi, D. M.; Prato, M. *Acc. Chem. Res.* **2000,** *33*, 695.